

# Adequacy of Approximations in $GW$ Theory

Mark van Schilfgaarde,<sup>1</sup> Takao Kotani,<sup>1</sup> and Sergey V. Faleev<sup>2</sup>

<sup>1</sup>*Arizona State University, Tempe, AZ, 85284*

<sup>2</sup>*Sandia National Laboratories, Livermore, CA 94551*

(Dated: February 8, 2020)

## Abstract

Following the usual procedure of the  $GW$  approximation ( $GWA$ ) within the first-principles framework, we calculate the self energy from eigenfunctions and eigenvalues generated by the local-density approximation (LDA). We analyze several possible sources of error in the theory and its implementation, using a recently development all-electron method approach based on the full-potential linear muffin-tin orbital (LMTO) method. First we present some analysis of convergence in some quasiparticle energies with respect to the number of bands, and also their dependence on different basis sets within the LMTO method. We next present a new analysis of core contributions. Then we apply the  $GWA$  to a variety of materials systems, to test its range of validity. For simple  $sp$  semiconductors,  $GWA$  always underestimates bandgaps. Better agreement with experiment is obtained when the renormalization ( $Z$ ) factor is not included, and we propose a justification for it. We close with some analysis of difficulties in the usual  $GWA$  procedure.

## I. INTRODUCTION

Even though the  $GW$  approximation ( $GWA$ ) of Hedin<sup>1</sup> is as old as the local-density approximation (LDA), it is still in its early stages because of serious difficulties in its implementation. In the usual *ab initio* procedure,  $G$  and  $W$  are constructed from the LDA potential, which generate the self-energy  $\Sigma = iG \times W$ . Additionally the quasiparticle energies (QPE) are usually approximated as a perturbation correction to the LDA, from the matrix elements of the diagonal parts of  $\Sigma - V_{xc}^{LDA}$ ; see Eqns. 18 and 19 below. In principle, it is well-defined as a procedure. However, there is a controversy what the numerical result of this procedure is for semiconductors. Nearly always the  $GWA$  is implemented in conjunction with the pseudopotential (PP) approximation, which we will call PPGW. It was widely thought that PPGW predicts bandgaps in semiconductors to rather high accuracy. However, recent all-electron  $GW$  calculations to survey bandgaps in semiconductors using the full-potential LMTO (FP-LMTO) by Kotani and van Schilfgaarde<sup>2</sup> result in bandgaps that are generally smaller than experimental values. The result is confirmed by other calculations using two independently-developed full-potential linear augmented plane wave (FP-LAPW) codes: one by Usuda, Hamada, Kotani and van Schilfgaarde<sup>3</sup> and another by Friedrich, Schindlmayr, Blügel and Kotani<sup>4</sup>. These methods all use essentially the same  $GW$  codes originally developed in conjunction with the LMTO method<sup>2</sup>; they differ only in the input eigenfunctions. Calculations from other, independently developed all-electron  $GW$  methods<sup>5,6,7</sup> are consistent with this conclusion<sup>8</sup>.

Tiago, Ismail-Beigi, and Louie<sup>9</sup> used the PPGW scheme that included Si 2s and 2p cores in the valence to analyze the dependence of some semiconductor bandgaps on the number of unoccupied states  $N'$  used to construct the self-energy. They suggested that the discrepancy between all-electron  $GW$  and PPGW gaps could be attributed to incomplete convergence in the all-electron calculations. To address this point, the convergence in  $N'$  is taken up in Sec. III. We begin with an outline our all-electron  $GW$  method (Sec. II); it includes a comparison of the energy bands in Si to those of an APW calculation taken from Friedrich et al.<sup>4</sup>, establish the method's ability to reproduce near-exact LDA eigenvalues. In Sec. IV we show how selected QPEs change with increasingly larger LMTO basis sets for a variety of semiconductors. The results are weakly dependent on basis even for relatively small basis sets. We present some rationale for why this should be so, and note the implications for

both precision and efficiency in implementations of the *GWA* for basis sets in general.

Because our results are well converged for either kind of test, we still think that *PPGW* is problematic, in contradistinction to the conclusions in a recent paper by Delaney, García-González, Rubio, Rinke and Godby<sup>10</sup>, who showed that all-electron *GW* and *PPGW* give essentially the same result for the Be free atom. However, the Be atom is a special case in part because the all-electron and pseudo radial functions should closely correspond to each other (the  $2p$  radial function has no nodes, and the only core that is orthogonalized or pseudized is the deep  $1s$  core ( $\epsilon^{\text{LDA}} \approx -105$  eV); moreover the PP is constructed with the atom itself as reference. Pseudopotentials are constructed to solve LDA reliably, but not to solve the *GWA*. There are now many detailed checks comparing PP-LDA results against the corresponding all-electron values; but there are few similar comparisons for *GW*. The discrepancies between all-electron and *PPGW* appear to be much smaller when *PPGW* includes the highest lying core states in the valence.

Sec. V analyzes different core contributions to the QPE in several semiconductors. This provides some insight as to what approximations may be made concerning the core; we also briefly consider some aspects of *PPGW* in this context.

In Sec. VI we show some new results for a variety of materials, as well as repeating some previously reported calculations<sup>2,11,12,13,14</sup> with rather tight tolerances. We confirm that the usual *GWA* procedure generally underestimates bandgaps. We also show that a partial self-consistency can be accomplished by calculating QPEs without the renormalization factor  $Z$  (i.e.  $Z = 1$ ). Semiconductor bandgaps are systematically improved using  $Z = 1$ , though they continue to be underestimated. An important reason for this is that the LDA overestimates the screening of  $W$ , resulting in an underestimate of  $\Sigma = iGW$  and bandgaps. We show that the adequacy of the *GWA* varies from system to system: only when the starting LDA is reasonably good does the *GWA* reasonably predict QP energies. Thus, some kind of self-consistency is necessary to obtain reasonable results for wide range of materials.<sup>12</sup>

## II. METHODOLOGY

### All-electron LDA in FP-LMTO

Before turning to the analysis, we briefly describe the LDA method we use as input for the *GW* calculations. (Readers interested in conclusions of this paper *not* related to basis-set issues can skip this section). An early version of this method was presented in Ref. 15; we describe here how additional local orbitals are included to extend the linear method. Local orbitals are essential to the analysis, because QPE in *GWA* are sensitive to a wider range of states than in LDA (e.g., the LDA depends only on occupied states). One consequence is that the linear approximation inherent in standard linear and pseudopotential methods is less reliable for the *GWA* than for the LDA. The basis functions used in the present technique are a generalization<sup>15</sup> of the standard<sup>16</sup> method of linear muffin-tin orbitals (LMTO). Conventional LMTOs consist of atom-centered envelope functions augmented around atomic sites by a linear combination of radial wave functions  $\varphi$  and their energy derivatives  $\dot{\varphi}$ .  $\varphi = \varphi_{Rl}(\varepsilon_{Rl}, r)$  is the solution of radial Schrödinger equation at site  $R$  at some linearization energy  $\varepsilon_{Rl}$ . A linear method matches the  $\{\varphi, \dot{\varphi}\}$  pair to value and slope of the envelope function at each augmentation sphere boundary, which means that the LDA Schrödinger equation can be solved more or less exactly to first order in  $\varepsilon - \varepsilon_{Rl}$  inside each augmentation sphere. Envelope functions in the standard LMTO method consist of Hankel functions. In the present basis<sup>15</sup> the envelope functions are smooth, nonsingular generalizations<sup>17</sup> of the Hankel functions: the  $l=0$  smooth Hankel satisfies the equation

$$\begin{aligned} (\nabla^2 + \varepsilon)H_0(\varepsilon, r^s; \mathbf{r}) &= -4\pi g_0(r^s, r) \\ g_0(r^s; r) &= \left(\sqrt{\pi}r^s\right)^{-3} \exp\left(-(r/r^s)^2\right) \rightarrow \delta(\mathbf{r}) \text{ as } r^s \rightarrow 0 \end{aligned} \quad (1)$$

and reduces to a usual Hankel function in the limit  $r^s \rightarrow 0$ .  $H_L$  for higher  $L=(l, m)$  are obtained by recursion<sup>17</sup>. The basis can be divided into three types of functions:

(i) A muffin-tin orbital (MTO)  $\chi_{RjL}$  which consists of a smoothed Hankel centered at nucleus  $\mathbf{R}$  and augmented by linear combinations of  $\varphi_{Rl}$  and  $\dot{\varphi}_{Rl}$  for each  $L$  channel inside every augmentation sphere

$$\chi_{RjL}(\mathbf{r}) = H_L(\varepsilon_{Rjl}, r_{Rjl}^s; \mathbf{r} - \mathbf{R}) + \sum_{R'k'L'} C_{R'k'L'}^{RjL} \{\tilde{P}_{R'k'L'}(\mathbf{r}) - P_{R'k'L'}(\mathbf{r})\} \quad (2)$$

$P_{R'k'L'}$  is a one-center expansion of  $H_L(\varepsilon_{Rjl}, r_{Rjl}^s; \mathbf{r} - \mathbf{R})$ , and  $\tilde{P}_{R'k'L'}$  is a linear combination of  $\varphi_{Rl}(\varepsilon_{Rjl}, r)$  and  $\dot{\varphi}_{Rl}(\varepsilon_{Rjl}, r)$  that matches  $P_{R'k'L'}$  at the augmentation sphere radius. Expansion coefficients  $C_{R'k'L'}^{RjL}$  are chosen to make  $\chi_{RjL}(\mathbf{r})$  smooth across each augmentation boundary.  $\varepsilon_{Rjl}$  is chosen to be at or near the center of the occupied part of that particular  $l$  channel. Products of such functions enters into the construction of the hamiltonian and output density. The present method differs in significant ways from the usual LMTO and LAPW methods, and is not a simple product of MTO Eq. (2), and bears some resemblance to the Projector Augmented Wave prescription<sup>18</sup>. It greatly facilitates  $l$  convergence in the augmentation; see Ref. 15.

(ii) “Floating orbitals” consisting of the same kind of function as (i), but not centered at a nucleus. Thus, there is no augmentation sphere where the envelope function is centered. There is no fundamental distinction between this kind of function and the first type, except that the distinction is useful when analyzing convergence. Floating orbitals make little difference in LDA calculations; but a basis consisting of purely atom centered envelope functions is not quite sufficient to precisely represent the interstitial over the wide energy window needed for  $GW$  calculations. Without their inclusion, errors in QPE of order 0.1 eV cannot be avoided, as we will show.

(iii) A kind of “local orbital” which has a structure similar to (i). The fundamental distinction is that the “head” (site where the envelope is centered) consists of a new radial function  $\phi_l^z$  evaluated at energy  $\varepsilon_l^z$  either far above or far below the linearization energy  $\varepsilon_l$ . For deep, core-like orbitals  $\phi_l^z$  is integrated at the core energy; for high-lying orbitals  $\varepsilon_l^z$  is typically taken 1-2 Ry above the Fermi level  $E_F$ . In the former case a tail is attached, with its smoothing radius  $r^s$  chosen to make the kinetic energy continuous across the “head” augmentation sphere. It is thus atypical of conventional local orbitals, as it is nearly an eigenstate of the LDA hamiltonian without requiring other basis functions.

As is well known, the reason for using augmented wave methods in general (and especially the LMTO method), is that the Hilbert space of eigenfunctions in the energy range of interest is spanned by much fewer basis functions than with other basis sets. In the present method two envelope functions  $j = 1, 2$  are typically used for low  $l$  channels  $s$ ,  $p$ , and  $d$ , and one for higher  $l$  channels ( $f$  and sometimes  $g$ ). The augmentation + local orbital procedure ensures that the basis is reasonably complete inside each augmentation sphere within a certain

energy window; the envelope functions + floating orbitals ensures completeness of the basis in the interstitial. The distinction between standard LMTO envelope functions and the smoothed ones used here is important because the generalized form significantly improves this convergence. Core states not treated as local orbitals are handled by integrating the radial Schrödinger equation inside an augmentation sphere and attaching a smoothed Hankel tail, allowing it to spill into the interstitial. Thus the Hartree and exchange correlation potentials are properly included; only the matrix element coupling core and valence states is neglected.

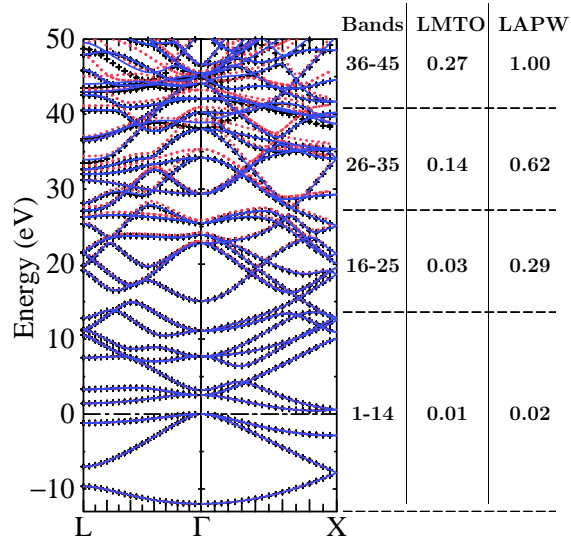


FIG. 1: LDA energy bands in Si, computed by different methods. APW bands from Ref. 19 are denoted by “+” and can be regarded as near exact. Dots denote bands calculated by the same authors using the LAPW method, without local orbitals. Solid lines denote bands computed by the present generalized LMTO method, including local and floating orbitals as described in the text (180 energy bands were included in the basis). On the right is a table of the RMS deviation relative to the APW bands for several energy windows, computed along the L– $\Gamma$  line. First column denotes the range of bands used to compute the RMS deviation; the horizontal dashed lines denote the approximate energy window for each range. Second and third columns denote the how the present method and the LAPW method respectively deviate from the APW bands, in eV, as described in the text.

When used in conjunction with  $GW$  calculations we typically add local orbitals for states not spanned by  $\{\phi, \dot{\phi}\}$ , and whose center of gravity falls within  $\sim \pm 25$  eV of the Fermi level

$E_F$ . Both the low-lying and high-lying states can be important, and we shall return to it later. Fig. 1 shows the effects of linearization in Si, where an APW calculation of the LDA energy bands is available<sup>19</sup>. Friedrich et al.<sup>19</sup> compared LDA bands generated by a full APW calculation to those generated by LAPW. They are reproduced in Fig. 1, together with the bands generated by the LMTO+local+floating orbitals described above. The LAPW and APW are nearly indistinguishable on the scale of figure for energies up to  $\sim 25$  eV. For energies above 25 eV, the LAPW begins to deviate from the other two, showing the effects of linearization. The APW and generalized LMTO bands are essentially indistinguishable on the scale of figure for energies up to  $\sim 40$  eV. Above that, slight differences begin to appear; the differences gradually increase for still higher energies. Fig. 1 also tabulates the RMS deviation from the APW bands for several energy windows. The present method agrees with the APW bands to  $\sim 0.01$  eV for levels within  $E_F \pm 1\text{Ry}$ , and to  $\sim 0.25$  eV for levels below  $E_F + 4\text{Ry}$ . Friedrich et al. report similar improvements to their LAPW bands when local orbitals are added<sup>4</sup>. They also compare bands generated by a PP, and show that the errors are comparable to the conventional LAPW method. Fig. 1 establishes rather convincingly that the present method is nearly complete over a rather wide energy window in Si. When local orbitals are included, it is comparable to an LAPW method that includes local orbitals<sup>19</sup>, and it is superior both to PP and conventional LAPW methods.

### All-electron $GW$ with mixed basis for $W$

We briefly describe our all-electron implementation of the  $GW$  approximation. A more detailed account will be given elsewhere<sup>20</sup>. The self-energy  $\Sigma$  is

$$\Sigma(\mathbf{r}, \mathbf{r}', \omega) = \frac{i}{2\pi} \int d\omega' G(\mathbf{r}, \mathbf{r}', \omega - \omega') e^{i\delta\omega'} W(\mathbf{r}, \mathbf{r}', \omega'). \quad (3)$$

In this paper  $G$  will be taken to be the one-body non-interacting Green function as computed by the LDA, and the screened Coulomb interaction  $W$  is computed in the random-phase approximation (RPA) from  $G$ . Both  $G$  and  $W$  are obtained from the LDA eigenvalues  $\varepsilon_{\mathbf{k}n}$  and eigenfunctions  $\Psi_{\mathbf{k}n}$ . For a periodic hamiltonian, we can restrict  $\mathbf{r}$  and  $\mathbf{r}'$  to a unit cell and write  $G$  as

$$G_{\mathbf{k}}(\mathbf{r}, \mathbf{r}', \omega) = \sum_n^{\text{All}} \frac{\Psi_{\mathbf{k}n}(\mathbf{r}) \Psi_{\mathbf{k}n}^*(\mathbf{r}')}{\omega - \varepsilon_{\mathbf{k}n} \pm i\delta}. \quad (4)$$

The infinitesimal  $-i\delta$  is to be used for occupied states, and  $+i\delta$  for unoccupied states.  $W$  is written as

$$W = \epsilon^{-1}v = (1 - v\Pi)^{-1}v \quad (5)$$

where  $\Pi = -iG \times G$  is the bare polarization function shown below,  $v = e^2/|\mathbf{r} - \mathbf{r}'|$  is the bare coulomb interaction, and  $\epsilon$  is the dielectric function. For simplicity, the spin degree of freedom is omitted.

Neglecting the off-diagonal part of  $\Sigma$ , we can evaluate QPE  $E_{\mathbf{kn}}$  from

$$E_{\mathbf{kn}} = \varepsilon_{\mathbf{kn}} + Z_{\mathbf{kn}}[\langle \Psi_{\mathbf{kn}} | \Sigma(\mathbf{r}, \mathbf{r}', \varepsilon_{\mathbf{kn}}) | \Psi_{\mathbf{kn}} \rangle - \langle \Psi_{\mathbf{kn}} | V_{\text{xc}}^{\text{LDA}}(\mathbf{r}) | \Psi_{\mathbf{kn}} \rangle]. \quad (6)$$

$Z_{\mathbf{kn}}$  is the quasi-particle (QP) renormalization factor

$$Z_{\mathbf{kn}} = \left[ 1 - \langle \Psi_{\mathbf{kn}} | \frac{\partial}{\partial \omega} \Sigma(\mathbf{r}, \mathbf{r}', \varepsilon_{\mathbf{kn}}) | \Psi_{\mathbf{kn}} \rangle \right]^{-1}, \quad (7)$$

and accounts for the fact that  $\Sigma$  is evaluated at the LDA energy rather than at the QPE. Eq. (6) is the customary way QPEs are evaluated in *GW* calculations. In Sec. VI, we present an argument that using  $Z = 1$  (or neglecting the  $Z$  factor) is a better choice than Eq. (7), and how the QPE is affected in actual calculations. However, the results presented here use the  $Z$  factor except where noted.

In FP-LMTO, eigenfunctions of the valence states are expanded in linear combinations of Bloch summed MTOs, Eq. (2)

$$\Psi_{\mathbf{kn}}(\mathbf{r}) = \sum_{RjL} a_{RjL}^n \chi_{RjL}^{\mathbf{k}}(\mathbf{r}), \quad (8)$$

Inside augmentation sphere  $\mathbf{R}$ , the Hilbert space of the valence eigenfunction  $\Psi_{\mathbf{kn}}(\mathbf{r})$  consists of the pair (or triplet) of orbitals  $(\varphi_{Rl}, \dot{\varphi}_{Rl}$  or  $\varphi_{Rl}, \dot{\varphi}_{Rl}, \varphi_{Rl}^z)$  at that site<sup>21</sup>, and can be represented in a compact notation  $\{\varphi_{Ru}\}$ .  $u$  is a compound index for both  $L$  and one of the  $(\varphi_{Rl}, \dot{\varphi}_{Rl}, \varphi_{Rl}^z)$  triplet. The interstitial is comprised of linear combinations of envelope functions consisting of smooth Hankel functions, which can be expanded in terms of plane waves<sup>17</sup>. Therefore the  $\Psi_{\mathbf{kn}}(\mathbf{r})$  can be written as a sum of augmentation and interstitial parts

$$\Psi_{\mathbf{kn}}(\mathbf{r}) = \sum_{Ru} \alpha_{Ru}^{\mathbf{kn}} \varphi_{Ru}^{\mathbf{k}}(\mathbf{r}) + \sum_{\mathbf{G}} \beta_{\mathbf{G}}^{\mathbf{kn}} P_{\mathbf{G}}^{\mathbf{k}}(\mathbf{r}), \quad (9)$$



where the interstitial plane wave (IPW) is defined as

$$\begin{aligned} P_{\mathbf{G}}^{\mathbf{k}}(\mathbf{r}) &= 0 \quad \text{if } \mathbf{r} \in \text{any MT} \\ &= \exp(i(\mathbf{k} + \mathbf{G})\mathbf{r}) \quad \text{otherwise,} \end{aligned} \quad (10)$$

and the  $\varphi_{Ru}^{\mathbf{k}}$  are Bloch sums of  $\varphi_{Ru}$

$$\varphi_{Ru}^{\mathbf{k}}(\mathbf{r}) \equiv \sum_{\mathbf{T}} \varphi_{Ru}(\mathbf{r} - \mathbf{R} - \mathbf{T}) \exp(i\mathbf{k} \cdot \mathbf{T}). \quad (11)$$

$\mathbf{T}$  and  $\mathbf{G}$  are lattice translation vectors in real and reciprocal space, respectively.

Throughout this paper, we will designate eigenfunctions constructed from MTOs as “VAL”. Below them are the core eigenfunctions which we designate as “CORE”. There are two fundamental distinctions between VAL and CORE eigenfunctions: the latter are constructed independently by integration of the spherical part of the LDA potential, and they are not included in the secular matrix. Second, the cores are confined to MT spheres<sup>22</sup>. CORE eigenfunctions are also expanded using Eq. (9) in a trivial manner;  $\beta_{\mathbf{G}}^{\mathbf{k}n} = 0$  and only one of  $\alpha_{Ru}^{\mathbf{k}n} \neq 0$ . The discussion below applies to all eigenfunctions, VAL and CORE.

Through Eq. (9), products  $\Psi_{\mathbf{k}_1 n} \times \Psi_{\mathbf{k}_2 n'}$  can be expanded by  $P_{\mathbf{G}}^{\mathbf{k}_1 + \mathbf{k}_2}(\mathbf{r})$  in the interstitial region because  $P_{\mathbf{G}_1}^{\mathbf{k}_1}(\mathbf{r}) \times P_{\mathbf{G}_2}^{\mathbf{k}_2}(\mathbf{r}) = P_{\mathbf{G}_1 + \mathbf{G}_2}^{\mathbf{k}_1 + \mathbf{k}_2}(\mathbf{r})$ . Within sphere  $R$ , wave function products can be expanded by  $B_{Rm}^{\mathbf{k}_1 + \mathbf{k}_2}(\mathbf{r})$ , which is the Bloch sum of the product basis  $\{B_{Rm}(\mathbf{r})\}$ , which in turn is constructed from the set of products  $\{\varphi_{Ru}(\mathbf{r}) \times \varphi_{Ru'}(\mathbf{r})\}$  adapting the procedure by Aryasetiawan<sup>23</sup>. Eq. (9) is equally valid in a LMTO or LAPW framework, and eigenfunctions from both types of methods have been used in this  $GW$  scheme<sup>3,4</sup>. We restrict ourselves to LMTO-derived basis functions here.

We define the mixed basis  $\{M_I^{\mathbf{k}}(\mathbf{r})\} \equiv \{P_{\mathbf{G}}^{\mathbf{k}}(\mathbf{r}), B_{Rm}^{\mathbf{k}}(\mathbf{r})\}$ , where the index  $I \equiv \{\mathbf{G}, Rm\}$  classifies the members of the basis. By construction,  $M_I^{\mathbf{k}}$  is a good basis set for the expansion of products of  $\Psi_{\mathbf{k}n}$ . Complete information to calculate  $\Sigma$  and  $E_n(\mathbf{k})$  are matrix elements of the products  $\langle \Psi_{\mathbf{q}n} | \Psi_{\mathbf{q}-\mathbf{k}n'} M_I^{\mathbf{k}} \rangle$ , the LDA eigenvalues  $\varepsilon_{\mathbf{k}n}$ , the Coulomb matrix  $v_{IJ}(\mathbf{k}) \equiv \langle M_I^{\mathbf{k}} | v | M_J^{\mathbf{k}} \rangle$ , and the overlap matrix  $\langle M_I^{\mathbf{k}} | M_J^{\mathbf{k}} \rangle$ . (The overlap matrix of IPW is necessary because  $\langle P_{\mathbf{G}}^{\mathbf{k}} | P_{\mathbf{G}'}^{\mathbf{k}} \rangle \neq 0$  for  $\mathbf{G} \neq \mathbf{G}'$ .) The Coulomb interaction is expanded as

$$v(\mathbf{r}, \mathbf{r}') = \sum_{\mathbf{k}, I, J} |\tilde{M}_I^{\mathbf{k}}\rangle v_{IJ}(\mathbf{k}) \langle \tilde{M}_J^{\mathbf{k}}|, \quad (12)$$

where we define

$$|\tilde{M}_I^{\mathbf{k}}\rangle \equiv \sum_{I'} |M_{I'}^{\mathbf{k}}\rangle (O^{\mathbf{k}})_{II'}^{-1}, \quad (13)$$

$$O_{I'I}^{\mathbf{k}} = \langle M_{I'}^{\mathbf{k}} | M_I^{\mathbf{k}} \rangle. \quad (14)$$

$W$  and the polarization function  $\Pi$  shown below are expanded in the same manner as Eq. (12).

The exchange part of  $\Sigma$  is written in the mixed basis as

$$\langle \Psi_{\mathbf{q}n} | \Sigma_{\text{x}} | \Psi_{\mathbf{q}n} \rangle = \sum_{\mathbf{k}}^{\text{BZ}} \sum_{n'}^{\text{occ}} \langle \Psi_{\mathbf{q}n} | \Psi_{\mathbf{q}-\mathbf{k}n'} \tilde{M}_I^{\mathbf{k}} \rangle v_{IJ}(\mathbf{k}) \langle \tilde{M}_J^{\mathbf{k}} \Psi_{\mathbf{q}-\mathbf{k}n'} | \Psi_{\mathbf{q}n} \rangle. \quad (15)$$

The screened Coulomb interaction  $W_{IJ}(\mathbf{q}, \omega)$  is calculated through Eq. (5), where the polarization function  $\Pi$  is written

$$\begin{aligned} \Pi_{IJ}(\mathbf{q}, \omega) &= \sum_{\mathbf{k}}^{\text{BZ}} \sum_n^{\text{occ}} \sum_{n'}^{\text{unocc}} \langle \tilde{M}_I^{\mathbf{q}} \Psi_{\mathbf{k}n} | \Psi_{\mathbf{q}+\mathbf{k}n'} \rangle \langle \Psi_{\mathbf{q}+\mathbf{k}n'} | \Psi_{\mathbf{k}n} \tilde{M}_J^{\mathbf{q}} \rangle \\ &\times \left( \frac{1}{\omega - \varepsilon_{\mathbf{q}+\mathbf{k}n'} + \varepsilon_{\mathbf{k}n} + i\delta} - \frac{1}{\omega + \varepsilon_{\mathbf{q}+\mathbf{k}n'} - \varepsilon_{\mathbf{k}n} - i\delta} \right). \end{aligned} \quad (16)$$

Eq. (16) assumes time-reversal symmetry. We use the tetrahedron method for the Brillouin zone (BZ) summation in Eq. (16) following Ref. 24. We first calculate the contribution to  $\Pi$  proportional to the imaginary part of the second line in Eq. (16), and determine the rest of  $\Pi$  by Hilbert transformation (Kramers-Krönig relation). Such approach significantly reduces the computational time required to calculate  $\Pi$ .

The correlation part of  $\Sigma$  is

$$\begin{aligned} \langle \Psi_{\mathbf{q}n} | \Sigma_{\text{c}}(\omega) | \Psi_{\mathbf{q}n} \rangle &= \sum_{\mathbf{k}}^{\text{BZ}} \sum_{n'}^{\text{All}} \sum_{IJ} \langle \Psi_{\mathbf{q}n} | \Psi_{\mathbf{q}-\mathbf{k}n'} \tilde{M}_I^{\mathbf{k}} \rangle \langle \tilde{M}_J^{\mathbf{k}} \Psi_{\mathbf{q}-\mathbf{k}n'} | \Psi_{\mathbf{q}n} \rangle \\ &\times \int_{-\infty}^{\infty} \frac{id\omega'}{2\pi} W_{IJ}^{\text{c}}(\mathbf{k}, \omega') \frac{1}{-\omega' + \omega - \varepsilon_{\mathbf{q}-\mathbf{k}n'} \pm i\delta}. \end{aligned} \quad (17)$$

Here  $-i\delta$  is for occupied states;  $+i\delta$  is for unoccupied states.  $W^{\text{c}} \equiv W - v$ .

$GW$  calculations usually approximate Eq. (6) by

$$E_{\mathbf{k}n} = \varepsilon_{\mathbf{k}n} + Z_{\mathbf{k}n} [\langle \Psi_{\mathbf{k}n} | \Sigma^{\text{VAL}}(\mathbf{r}, \mathbf{r}', \varepsilon_{\mathbf{k}n}) | \Psi_{\mathbf{k}n} \rangle - \langle \Psi_{\mathbf{k}n} | V_{\text{xc}}^{\text{LDA}}([n^{\text{VAL}}], \mathbf{r}) | \Psi_{\mathbf{k}n} \rangle] \quad (18)$$

where  $\Sigma^{\text{VAL}}$  and  $V_{\text{xc}}^{\text{LDA}}([n^{\text{VAL}}])$  are calculated only from eigenfunctions belonging to VAL. In the present method we calculate the  $E_{\mathbf{k}n}$  including the core contributions from

$$\begin{aligned} E_{\mathbf{k}n} &= \varepsilon_{\mathbf{k}n} + Z_{\mathbf{k}n} \times [\langle \Psi_{\mathbf{k}n} | \Sigma_{\text{x}}(\mathbf{r}, \mathbf{r}') + \Sigma_{\text{c}}(\mathbf{r}, \mathbf{r}', \varepsilon_{\mathbf{k}n}) | \Psi_{\mathbf{k}n} \rangle \\ &\quad - \langle \Psi_{\mathbf{k}n} | V_{\text{xc}}^{\text{LDA}}([n^{\text{total}}], \mathbf{r}) | \Psi_{\mathbf{k}n} \rangle]. \end{aligned} \quad (19)$$

Note  $V_{xc}^{LDA}([n^{\text{total}}], \mathbf{r})$  is for entire density  $n^{\text{total}}$ . As  $n'$  in Eq. (15) can be divided between CORE and VAL, we have  $\Sigma_x = \Sigma_x^{\text{CORE}} + \Sigma_x^{\text{VAL}}$ . In this paper, we neglect the CORE contribution to  $\Sigma_c$ . In Sec. V we examine in some detail the contributions by shallow cores to correlation by including them in VAL using local orbitals, and will see that their contribution is small except for very shallow cores.

In short, no important approximation is made other than the  $GW$  approximation itself; and it is to the best of our knowledge the only implementation of  $GWA$  that makes no significant approximations. Results depend slightly on what kind basis set used to generate  $G$  and  $W$ , as we will show, and also on the tolerances in parameters used in the  $GW$ -specific part of the calculation.

LMTO-based calculations presented here employ a widely varying set of basis functions, ranging from  $\sim 20$ – $90$  orbitals per atom, as described in more detail below. They typically consist of a basis of *spdfg*+*spd* orbitals centered on each atom, some floating orbitals and sometimes local orbitals. In the Si calculations local  $p$  orbitals of either of  $2p$  character or of  $4p$  character were used, as we describe below. For the  $GW$  part of the calculation, the Si results shown below use parameters representative of the various system studied: LMTO basis functions are re-expanded in plane waves to a cutoff of  $3.3$  a.u. in the interstitial region, i.e.  $|\mathbf{k} + \mathbf{G}| < 3.3 \text{ Bohr}^{-1}$  in the second term of Eq. (9). The IPW part of the mixed basis used to expand  $v$ ,  $\Pi$ , and  $W$  used a cutoff  $|\mathbf{k} + \mathbf{G}| < 3.0 \text{ Bohr}^{-1}$ ; the product basis part consisted of  $90$ – $110$  Bloch functions/atom (we use different product basis for  $\Sigma_x^{\text{CORE}}$  and  $\Sigma_x^{\text{VAL}}$ ). Augmentation sphere radii were chosen so that spheres approximately touched but did not overlap, and the product basis functions entering into the mixed basis  $\tilde{M}$  in Eqns. (16) and (17) were expanded to  $l=5$ . In the calculation of Eq. (17) the poles of  $G$  were Gaussian broadened by  $\sigma=0.003$  or  $0.01$  Ry. These parameters correspond to rather conservative tolerances: tests at tighter tolerances in these parameters change the QPE by  $\sim 0.01$  eV. (Systematic checks were performed for each material studied.) The tetrahedron method was used for  $\Pi$  with a  $6 \times 6 \times 6$   $k$ -mesh (doubling the number of points in the energy denominator) except where noted. The same mesh is used to calculate  $\Pi$  and  $\Sigma$ . This  $k$  mesh is reasonably well converged, systematically overestimating conduction-band states by  $\sim 0.02$  eV in Si and similar semiconductors relative to the fully  $k$ -converged result.<sup>25</sup>

### III. CONVERGENCE IN QUASIPARTICLE ENERGIES: NUMBER OF UNOCCUPIED STATES

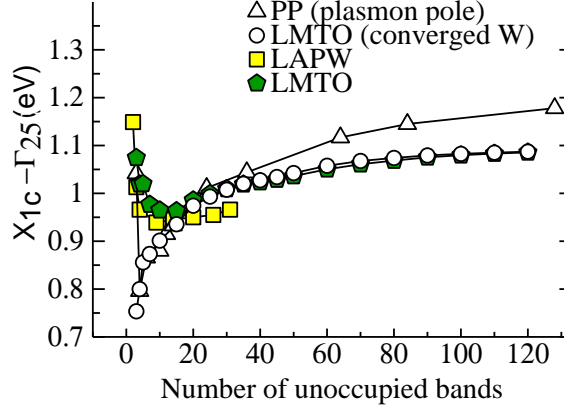


FIG. 2:  $\Gamma_{25v} \rightarrow X_{1c}$  gap in Si in GWA as a function of the number of unoccupied states  $N'$ . **Filled(Yellow) squares:** LAPW GWA taken from Ku and Eguiluz<sup>26</sup>. The authors presented data only for  $N' < 31$ . Also, their data was given for the minimum gap, so we shifted their results by +0.14 eV to estimate the  $\Gamma_{25v} \rightarrow X_{1c}$  gap. Some checks show that the shift should be  $\sim 0.14$  eV, approximately independent of  $N'$ . **Filled(Green) pentagons:** LMTO results varying  $N'$  both  $G$  and  $W$ . LMTO results were shifted by -0.02 eV to correct for incomplete  $k$  convergence<sup>25</sup>. The Si  $2p$  was included in the valence using a local orbital (the LAPW calculation of Ku and Eguiluz did not). The total dimension of the LMTO basis is 180. Results from the same basis are shown as Filled(green) pentagons in Fig. 4, and also Filled(green) pentagons No. (13) in Fig. 5. **Open triangles:** PPGW from Ref. 9, which included the Si  $2p$  levels as part of the valence, and in which  $W$  was computed using the plasmon-pole approximation. **Open circles:** LMTO results varying  $N'$  in  $G$  but not  $W$ .

In Fig. 2, we show the  $\Gamma_{25v} \rightarrow X_{1c}$  gap for Si computed by Eq. (19) as a function of the number of unoccupied states  $N'$  in Eqns. (16) and (17): i.e. summation  $n'$  over unoccupied states is restricted to  $n' < N'$ . Fig. 2 depicts our main with pentagons (Si  $2p$  treated as VAL). It tracks well the all-electron results of Ku and Eguiluz<sup>26</sup>, which used an LAPW method, except their data is  $\sim 0.05$  eV less than ours. However, their results are limited to  $N' < 31$ , which is not sufficient to analyze convergence for large  $N'$ . If one assumes the LAPW converges with  $N'$  at the same rate as the LMTO case, their best result with  $N' = 31$  should be  $\sim 0.1$  eV less than the converged value. Indeed a very recent calculation of the

same system by Friedrich, Schindlmayr, Blügel and Kotani<sup>4</sup>, based on LAPW with an LDA basis of  $\sim 300$  basis functions, showed  $N'$ -convergence similar to LMTO.

Tiago, Ismail-Beigi, and Louie<sup>9</sup> presented a PPGW calculation of some QPE in Si, Ge, and GaAs where they included the higher-lying core states into the valence so as to assess the effect of the core. They monitored the rate of convergence in QPE with  $N'$ ; their data for Si are shown as open triangles in Fig. 2. There are some similarities, but also two discrepancies:

- (i) For  $N' \lesssim 30$ , the behavior is rather different.
- (ii) In the asymptotic region  $N' \gtrsim 30$ , the PPGW and LMTO results converge at somewhat different rates.

In order to examine point (i), we tried LMTO calculations where  $W$  is fixed (i.e.  $N'$  is truncated only in Eq. (4)). This calculation (open circles in Fig. 2) tracks well the PPGW result for  $N' \lesssim 30$ . This looks reasonable because the PPGW is combined with the plasmon-pole approximation, which satisfies the sum rule for  $\text{Im} \epsilon^{-1}$  for any  $N'$ ; thus  $W$  converges rather quickly with respect to  $N'$ . However, the two LMTO calculations show little difference in the asymptotic behavior, which means that it is controlled by  $N'$  in Eq. (17), as was already discussed by Tiago et al.

It can be seen that the  $N'$  dependence of either LMTO calculation is slightly different than the PPGW result for both intermediate and large  $N'$ : the change in the  $\Gamma_{25v} \rightarrow X_{1c}$  gap from  $N' = 35$  to  $N' = 60$  for PPGW is roughly twice the change obtained by the LMTO method. As we noted in Sec. II, LMTO-LDA eigenvalues are very close to the full APW results in this energy range (see Fig. 1). This indicates that the eigenfunctions are also precise. Moreover, Friedrich et al.<sup>4</sup> compare LDA-APW eigenvalues to an LAPW+local orbitals method; the three sets of eigenvalues (APW and LMTO+local orbitals, LAPW+local orbitals) are very close to one another. By contrast, the LDA energy bands computed by either conventional LAPW or PP methods correspond to APW eigenvalues far less well; see Ref. 4. Finally, the dependence on  $N'$  as computed by the LAPW+local orbitals method is essentially similar to the present LMTO results. Taken together, these findings suggest that what discrepancy does exist between LMTO+local orbitals (or LAPW+local orbitals) and PPGW is likely to be an artifact of the PPGW method, even though the differences are small in absolute terms.

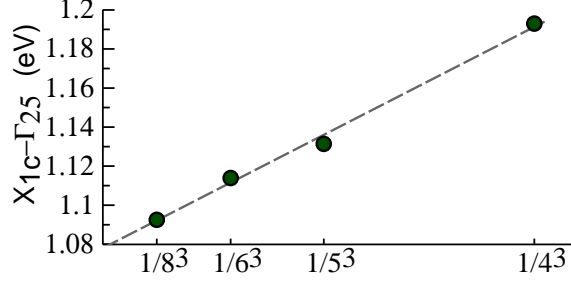


FIG. 3:  $\Gamma_{25v} \rightarrow X_{1c}$  gap in Si, as a function  $1/n_k^3$ , where  $n_k^3$  is the number of  $k$ -points in the full Brillouin zone. The dependence on  $1/n_k^3$  shown for  $\Gamma_{25v} \rightarrow X_{1c}$  is essentially same for all of the unoccupied QPEs we examined. Gaps for  $n_k=6$ ,  $n_k=5$ , and  $n_k=4$ , exceed the  $n_k=8$  case by 0.02 eV, 0.04 eV, and 0.10 eV, respectively. We can also estimate what the  $n_k \rightarrow \infty$  gap would be by extrapolating the approximately linear dependence on  $1/n_k^3$  to zero (dashed line). The  $n_k = 8$  case apparently overestimates the converged result by 0.01 eV.

It is also possible that the calculation by Tiago et al. suffers from incomplete  $k$ -convergence. Their PPGW used a  $4 \times 4 \times 4$   $k$ -mesh.  $k$ -convergence is mainly limited by divergent behavior for  $|\mathbf{k}| \rightarrow 0$  in Eq. 15. To treat this divergence, we use the offset- $\Gamma$  method, which was originally developed by ourselves<sup>2</sup> and is now used by other groups<sup>7,27</sup>. It is essentially equivalent to techniques that treat the divergent part analytically, as is typically done by PPGW practitioners. Fig. 3 shows the dependence of  $\Gamma_{25v} \rightarrow X_{1c}$  gap on  $n_k$ , but in general all of conduction bands shift nearly rigidly with changes in  $n_k$  ( $n_k$  = number of linear divisions of the  $k$ -mesh in the Brillouin zone). Bandgaps are approximately linear in the reciprocal of the total number of points,  $1/n_k^3$ . The figure shows that a  $4 \times 4 \times 4$   $k$ -mesh overestimates the  $k$ -converged gap by  $\sim 0.1$  eV<sup>25</sup>. This may explain most of the remaining discrepancy between the PPGW calculations of Tiago et al. and the present results.

In Sec. V we analyze the dependence of QPEs on the core treatment. Proper treatment of the core is somewhat subtle<sup>28</sup>, and we use the local orbitals for the analysis. Because they are already nearly exact solutions of the LDA for the states they constructed to represent, they minimally hybridize with other basis functions; consequently any higher lying CORE state can be readily be converted into a valence state with minimal perturbation of the LDA basis. Use of local orbitals enables us to investigate how different kinds of core contributions affect QPEs in a well-controlled and systematic way. We show that differing treatments of the Si 2*p* core only slightly affect QPEs; similar results are found for other deep cores. A

significantly larger dependence is apparently found using the PPGW method.

#### IV. CONVERGENCE IN QUASIPARTICLE ENERGIES: BASIS DEPENDENCE

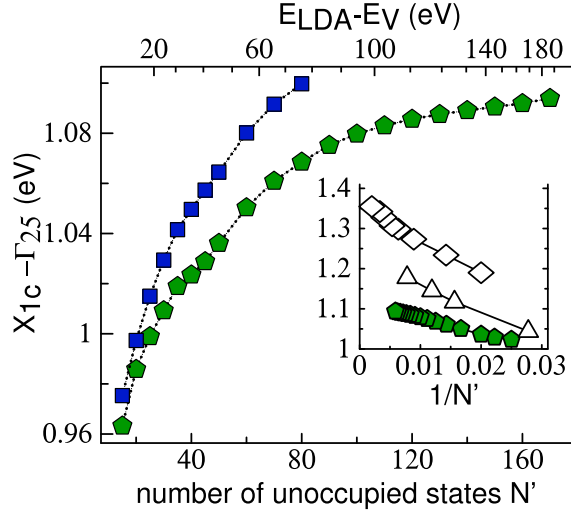


FIG. 4:  $\Gamma_{25v} \rightarrow X_{1c}$  gap in Si, as a function of number of unoccupied states  $N'$  for a smaller basis (squares) and a larger basis (pentagons). An approximate correspondence between the LDA energy  $\varepsilon_{\mathbf{k}n'}$  and  $N'$  is shown in the top scale. The latter are redrawn from Fig. 2. Top horizontal scale shows an approximate relation between energy and band index (interpolated from levels at  $\Gamma$  in the large basis). Inset compares convergence in  $X_{1c}$  as a function of  $1/N'$  to a PPGW calculation that includes  $2p$  states in the valence<sup>9</sup> (triangles) and a PPGW calculation that does not<sup>29</sup> (diamonds). LMTO data were shifted by  $-0.02$  eV to correct for incomplete  $k$  convergence<sup>25</sup>.

Here we study the convergence in QPEs as the LMTO basis set changes, retaining all the eigenfunctions for a given basis in the calculation ( $N'$  encompasses all unoccupied states). A given LMTO basis defines a finite Hilbert space of eigenfunctions; the  $GWA$  is a well-defined problem for that space, and we can study how the QPEs change as the Hilbert space is refined. This procedure corresponds more closely to analyses of basis set convergence common in other kinds of calculations (e.g. LDA and Hartree-Fock). We can also anticipate that it will be smoother than the  $N'$  truncation of Sec III; indeed this will turn out to be the case (see especially Fig. 5): the band gaps are insensitive to the choice of basis once a certain level of completeness is reached. It is also obviously true that the Hilbert space depends on the choice of basis constructing it. Therefore, the results presented here are specific to

the LMTO basis described in Sec. II, and in particular *what kinds* of orbitals are included, e.g. orbitals of  $f$  or  $g$  character, or local orbitals that correct the linearization inherent in most of the standard methods (LMTO, LAPW, and the construction of a norm-conserving PP). By adding different kinds of orbitals we can identify how different parts of the Hilbert space, (most notably corrections to linearization common to most methods) affect QPEs. Since the LMTO basis is tailored to the crystal potential, the LDA eigenfunctions converge more rapidly with the basis dimension than do plane-wave based basis sets<sup>30</sup>. Consequently we might expect a more rapid convergence in the *GWA* QPEs. On the other hand, by transformation to, e.g., Wannier functions, it should be possible to design a generic scheme that exhibits similarly rapid convergence.

Before presenting this analysis, we compare in Fig. 4 the dependence of the  $\Gamma_{25v} \rightarrow X_{1c}$  gap in Si on  $N'$  for two basis sets: one relatively small and another relatively large. For  $N' > 30$ , the gap rises much more rapidly with  $N'$  in the small-basis case. But the gap at the respective maximum  $N'$ —when  $N'$  includes all unoccupied states in each respective Hilbert space—are very similar. This suggests that the Hilbert space in both cases is sufficiently complete to determine the lowest excitation energy. We show in more detail below that this not merely an artifact of this particular pair of basis sets<sup>31</sup>.

Fig. 5 shows results of a systematic study of the convergence in the first unoccupied QPE at  $\Gamma$ , X, and L in Si with progressively larger basis sets. LDA eigenvalues are not shown because they are the same within  $\sim 0.01$  eV for all cases (0.60 eV for X, 1.42 eV for L, 2.52 eV for  $\Gamma$ ). These data comprise very diverse basis sets, particularly for the LMTO method which traditionally uses a minimal basis. Some details concerning these sets help explain in what manner convergence is reached:

§1 **Filled(yellow) diamonds (1)** includes *spdfsp* atom-centered functions, and is the only basis without floating orbitals. There are no local orbitals; Si  $1s, 2s, 2p$  are CORE.

§2 **Filled(blue) circles (2) and (3)** add floating orbitals of *sp* and of *spd* character, respectively. Their effect is to cause QPEs to *decrease* slightly relative to (1). Adding still more floating orbitals (even large numbers of them) shift QPEs by  $\sim 0.01$  eV.

§3 **Other Filled(blue) circles (5, 6, 10, 12)** include still more envelope functions comprised of a mixture of atom-centered functions and floating orbitals, but adding no local orbitals.



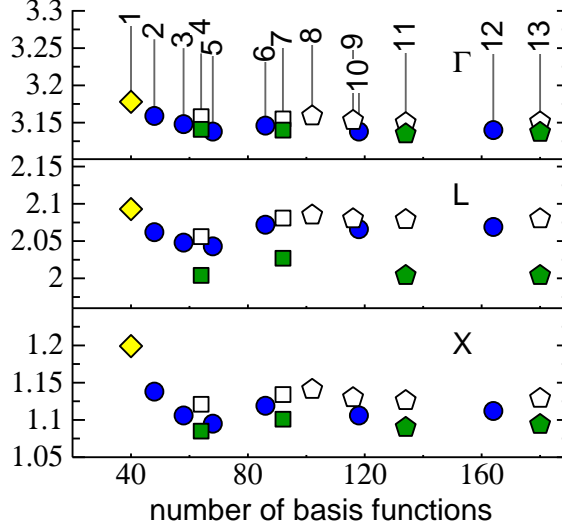


FIG. 5: QPE in the GWA at  $\Gamma_{15c}$  (top),  $L_{1c}$  (middle), and  $X_{1c}$  (bottom) in Si relative to the valence band maximum, using different basis sets in the present FP-LMTO. Abscissa is the total number of basis functions  $N$ . Yellow diamonds are a minimal basis (see text). All results depicted by fill circles contain no local orbitals. Those depicted by filled (empty) squares or pentagons include the Si  $2p$  (Si  $3p$ ) as local orbitals. See text for further description.

§4 **Filled(green) Square and Open Square (4, 7)** correspond to (3, 6), respectively, but adding a local orbital (Green: Si  $2p$ , Open: Si  $4p$ ). When the  $2p$  is included as VAL, CORE consists of Si  $1s, 2s$  only. A local orbital of *either* Si  $2p$  or Si  $4p$  shifts QPEs—in roughly equal but opposite directions.

§5 **Filled(green) Pentagon and Open Pentagon, (8,9,11,13)** include an additional Si  $4d$  local orbital. (11) corresponds to (10)+(Si  $2p$  or Si  $4p$ )+ Si  $4d$ . (13) corresponds to (12)+... as well. (8) is (6)+Si  $4p$ +Si  $4d$ . The effect of Si  $4d$  is small.

These points show in a compelling way that once the basis reaches a certain level of completeness, the change of QPE with further enlargement is very small. Set (1), which consists only of atom-centered functions, is somewhat incomplete except inside the augmentation spheres where the eigenfunctions are constructed out of linear combinations of  $\{\phi, \dot{\phi}\}$ . Considering the open structure of zincblende, such a basis may be expected to be less complete in the interstitial. Comparison basis sets without local orbitals (circles) with set (1) shows that this particular purely atom-centered basis is slightly deficient for reliable calculation of QPE, since the addition of floating orbitals induces a ( $k$ -dependent) reduction

in the conduction band of  $\sim 0.02 - 0.10$  eV. It is an open question whether a still more sophisticated atom-centered basis<sup>32</sup> would be adequate to describe the interstitial.

Once the interstitial is reasonably complete (*cf.* sets (3) and higher), there is an almost negligible dependence on basis *provided* no orbitals are included that extend the linear method or alter how the core is treated. Basis sets marked by a common symbol (squares, circles, pentagons) share essentially the same Hilbert space in the *augmentation* regions; only the basis set corresponding to the *interstitial* region changes. The variation is  $\pm 0.01$  eV for a wide range of basis sets<sup>31</sup>.

Fig. 5 also gives us some insight to the limitations of the linear method. Basis sets (3) and (4), which differ only in how the Si  $p$  channel is treated inside the augmentation region, affect QPEs more strongly than radically enlarging the Hilbert space of the envelope functions—compare (3) $\rightarrow$ (4) and (3) $\rightarrow$ (12). Envelope functions affect only the interstitial; they negligibly affect the Hilbert space of the augmentation region. For the latter it is largely irrelevant how many envelope functions are used—and consequently the size of  $N'$  entering into Eqns. (16) and (17). What *is* relevant is the completeness of  $\{\phi, \dot{\phi}\}$ , and results are independent of basis dimension provided that *the entire*  $\{\phi, \dot{\phi}\}$  Hilbert space is included. Said another way, the LMTO method is by design reasonably complete over a certain energy window in the augmentation spheres, more or less independent of the envelope functions. A similar story may be told for the interstitial: sets (3, 6, 10, 12) differ in the number of envelope functions by as much as a factor of three, but QPEs are unchanged within  $\pm 0.01$  eV. QPEs shift when  $\{\phi, \dot{\phi}\} \rightarrow \{\phi, \dot{\phi}, \phi^{4p}\}$  or  $\{\phi, \dot{\phi}\} \rightarrow \{\phi, \dot{\phi}, \phi^{2p}\}$ , essentially independently of the number of envelope functions (3 $\rightarrow$ 4, 6 $\rightarrow$ 7, 10 $\rightarrow$ 11, 12 $\rightarrow$ 13).

Table I shows three other materials (CdO, Ge, and GaAs). We can see (1) rapid convergence in QPEs as the basis is enlarged for a *fixed* set of augmentation functions; and (2) extensions to a linear augmentation affect QPEs in a manner approximately independent of the total dimension of the Hamiltonian. (In GaAs, both  $3d$  and  $4d$  must be included as VAL. If not, significant errors result<sup>2</sup>). We have tested a number of other materials as well, and these trends appear to be rather general. As might be expected, the number of basis functions needed to make the Hilbert space reasonably complete depends somewhat on the elements involved. The heavier atoms have larger radii and consequently slower  $l$ -convergence in the number of envelope functions needed; also  $d$  orbitals often play an important role. More orbitals are required to make the basis complete when heavier atoms are

TABLE I: QPEs of the first unoccupied state at  $\Gamma$ , L, and X, for different basis sets, in eV (relative to valence maximum). Columns  $n_a$ ,  $n_f$ , and  $n_l$  denote the number of atom-centered functions, the number of floating orbitals, and the number of local orbitals respectively. The hamiltonian dimension is the sum of these numbers. Experimental data are adjusted for spin-orbit coupling by adding 1/3 of the splitting in the  $\Gamma_{15}$  valence bands. The first four CdO basis sets are identical to the last four except for the addition of local orbitals in the O  $3p$  and Cd  $5d$  channels. A  $6 \times 6 \times 6$   $k$ -mesh was used in these calculations.

Data type	$n_a$	$n_f$	$n_l$	$\Gamma$	L	X
CdO						
Expt+0				0.84		
LDA	59	18	12	-0.53	4.26	3.58
GW	59	18	12	0.14	5.18	4.97
	59	50	12	0.10	5.14	4.92
	82	66	12	0.10	5.16	4.89
	82	82	12	0.10	5.16	4.88
	59	18	3	-0.01	5.05	4.78
	59	50	3	-0.06	5.01	4.73
	82	66	3	-0.02	5.05	4.73
	82	82	3	-0.02	5.06	4.74
Ge						
Expt+0.10				1.00	0.88	1.20
LDA	50	18	10	-0.12	0.07	0.65
GW	50	18	10	0.80	0.65	0.94
	68	18	10	0.84	0.68	0.97
	82	50	10	0.83	0.67	0.96
	82	82	10	0.82	0.67	0.96
GaAs						
Expt+0.11				1.63	1.96	2.11
LDA	42	18	6	0.34	0.86	1.34
GW	42	18	6	1.44	1.68	1.79
	68	18	6	1.46	1.69	1.79
	82	50	6	1.44	1.66	1.77
	82	82	6	1.43	1.66	1.77
	82	82	11	1.43	1.68	1.81

involved.

As noted, the linear  $\{\phi, \dot{\phi}\}$  Hilbert space is already reasonably complete in the case of Si. But this is not true in general: oxides and nitrides form a materials class where the effect is significantly larger. CdO is one such example (CdO forms in the NaCl structure; the valence band maximum falls at L and the conduction band minimum falls at  $\Gamma$ .) As happens for Si, there is a weak dependence on basis when the number of envelope functions is changed and the Hilbert space of the augmentation is held constant. But the QPEs change by  $\sim 0.15 \pm 0.05$  eV when the O  $3p$  and Cd  $5d$  states are added, as Table I shows. (In this particular case it is the O  $3p$  contribution that is dominant; however, cases arise when the contributions from high-lying  $d$  or  $f$  orbitals can be of order  $1 - 2$  eV. NiO is such a case<sup>11</sup>.)

The inset of Fig. 4 shows some PPGW results for reference. Based on the observation that cutoff in the Hilbert space should be important, PPGW data by Tiago et al. should be extrapolated to  $1/N' \rightarrow 0$  because they used a very large LDA basis.

## V. CORE CONTRIBUTIONS TO $\Sigma_c$

In a series of papers, Shirley and co-workers analyzed the effects of the core on QPE in atoms (Shirley, Mitás and Martin, Ref. 33, Shirley and Martin, Ref. 34) semiconductors (Shirley, Zhu and S. G. Louie<sup>35,36</sup>) within the pseudopotential framework. Approximate core contributions to both Eq. (16) and (17) were evaluated. They also compared pseudopotentials constructed from both LDA exchange and from Hartree-Fock (HF) exchange for atoms and molecules<sup>37</sup>, and incorporated pseudopotentials of both types in studying core effects<sup>35,36</sup>. They found sizable shifts in QPE in Si, and rather dramatic and  $k$ -dependent shifts in Ge and GaAs. These analyses highlight the importance of core effects. However, the decomposition of the various core contributions in Ref. 36 is somewhat involved, and it is rather closely tied to the pseudopotential construction that was a part of their implementation. This makes it a little difficult to disentangle the various contributions.

Here we examine contributions from the shallowest cores to  $\Sigma_c$  within the framework of our  $GW$ . As we noted, all the eigenfunctions are divided into two groups CORE and VAL as explained in Sec. II. Using local orbitals we can represent the shallowest cores in VAL. To distinguish true core effects from artifacts of implementation<sup>28</sup>, we include these cores in the valence with local orbitals and treat them in a special way, as described below. We

denote such eigenfunctions as *core*, and the rest as *val*. Thus we distinguish three kinds of orbitals: CORE, *core*, and *val*:

$$\begin{array}{ccc}
 & \text{All eigenfunctions} & \\
 & \swarrow \quad \searrow & \\
 \text{CORE} & & \text{VAL} \\
 & \swarrow \quad \searrow & \\
 & \text{core} \quad \text{val} &
 \end{array} \tag{20}$$

In Si, for example, we use: CORE={1*s*, 2*s*}, *core*={2*p*} and *val*={3*s*, 3*p*, 3*d*, ...}. Because the *core* states are well separated from higher lying states, *G* can be partitioned into  $G = G^{\text{CORE}} + G^{\text{core}} + G^{\text{val}}$ .  $\Sigma_x$  is always calculated from the entire *G*, while  $\Sigma_c$  is calculated from *core* and *val* only (we do not consider any case where some portion of the self-energy is supplied by the LDA):  $\Sigma_c = i(G^{\text{core}} + G^{\text{val}})W^c$ , where  $W^c = W[\Pi] - v$ , and  $\Pi$  is calculated from  $G^{\text{core}} + G^{\text{val}}$ . Thus *core* states contribute to  $\Sigma_c$  directly through *G* in  $iGW^c$ , and also through  $W^c$ . We resolve these contributions; that is, we calculate  $\Sigma_c$  in one of four ways:

- (i) neglect the *core* contribution to  $\Sigma_c$  entirely: i.e.  $\Sigma_c = iG^{\text{val}}(W[\Pi^{\text{val}}] - v)$ , where  $W[\Pi^{\text{val}}]$  means that  $\Pi$  is calculated from  $G^{\text{val}}$  only. We denote this as “exchange-only *core*”.
- (ii) neglect the *core* contribution to screening :  $\Sigma_c = i(G^{\text{core}} + G^{\text{val}})(W[\Pi^{\text{val}}] - v)$ .
- (iii) neglect the *core* contribution to *G*:  $\Sigma_c = iG^{\text{val}}(W[\Pi] - v)$ .
- (iv)  $\Sigma_c = i(G^{\text{core}} + G^{\text{val}})(W[\Pi] - v)$ : there is no distinction between *core* and *val* states.

Table II shows that the difference between exchange-only (i) and *GW* (iv) approximations to core treatment is small in Si ( $\sim 0.03$  eV for  $X_{1c}$ ). As expected, the adequacy of an exchange-only core depends on how deep the core is. The exchange-only approximation for shallow cores, such as the Ga 3*d* and In 4*d*, and the highest lying *p* core in the column I (Na, K, Rb) and column IIA alkali metals (Mg, Ca, and Sr), is rather crude. It is interesting that the core contributions to  $\Pi$  and to *G* are *not* always additive.

The difference between (iii) and (iv) is in general rather small; that is, inclusion of *core* contributions of  $\Pi$  alone is sufficient to bring QPE results within 0.05 eV of the full results in Table II except for the very shallow Ga 3*d* channel. For moderately deep cores, exchange-only treatment (i) is generally adequate, as Aryasetiawan suggested. A rough rule of thumb

TABLE II: QPE of the first unoccupied state at  $\Gamma$ , L, and X relative to top of valence, for core treatments (i) – (iv) as described in the text, in eV. States and corresponding eigenvalues  $\varepsilon_c^{\text{LDA}}$  treated as *core* are:  $2p$  in Si,  $3d$  in Ga and Ge, and  $2s$  in Mg. Si data corresponds to basis set (13) in Fig. 5; GaAs data corresponds to the 68+18+6-orbital basis in Table I; Ge data corresponds to the 68+18+10-orbital basis in that table. Here  $G$  means  $(G^{\text{core}} + G^{\text{val}})$ ,  $W$  means  $W[\Pi]$  (see text). A  $6 \times 6 \times 6$   $k$ -mesh was used in these calculations. For results with better  $k$ -convergence and larger basis sets, see Table III.

	$\varepsilon_c^{\text{LDA}}$	(i) : $G^{\text{val}}, W[\Pi^{\text{val}}]$			(ii) : $G, W[\Pi^{\text{val}}]$			(iii) : $G^{\text{val}}, W$			(iv) : $G, W$		
		$\Gamma$	L	X	$\Gamma$	L	X	$\Gamma$	L	X	$\Gamma$	L	X
Si	-89.6	3.17	2.09	1.14	3.17	2.09	1.14	3.17	2.06	1.15	3.16	2.02	1.11
Ge	-24.7	0.98	0.74	0.98	0.96	0.73	0.95	0.88	0.71	0.99	0.84	0.68	0.97
GaAs	-14.8	1.65	1.83	1.86	1.63	1.82	1.85	1.54	1.75	1.83	1.46	1.69	1.79
MgO	-71.4	7.31	10.55	11.62	7.36	10.56	11.62	7.30	10.55	11.60	7.36	10.55	11.60

seems to be: for cores whose total charge  $Q_{\text{spill}}$  outside the augmentation radius is less than 0.01 electrons, exchange-only treatment of them results in errors  $\sim 0.1$  eV or less for the lowest excited states. (This radius may be taken as approximately half the nearest-neighbor bond length).

Inclusion of core contributions to  $\Pi$  can significantly increase the computational cost (in the Si case, leaving out the  $2p$  contribution to  $\Pi$  reduces the computational cost by  $\sim 40\%$ ). The relative smallness of corrections to exchange-only treatment, and the observation that core contributions to  $\Pi$  alone are adequate for all but the most shallow cores, suggests that a simple approximate inclusion of core contributions to  $\Pi$ , Eq. (16), should be adequate for all but the most shallow cores such as the Ga  $3d$ . (Fleszar and Hanke proposed a construction for pseudopotentials when core states are not pseudized<sup>38</sup>.) Supposing the core were confined to the augmentation sphere at site  $R$ , we can eliminate all contributions to the matrix element  $\langle \tilde{M}_I^{\mathbf{q}} \Psi_{\mathbf{k}n} | \Psi_{\mathbf{q}+\mathbf{k}n'} \rangle$  except from the product-basis contribution at  $R$ . Since also the augmented part of  $\Psi$  depends rather weakly on  $\dot{\varphi}_{RI}$  we can neglect the  $\dot{\varphi}_{RI}$  contribution to the eigenfunctions and assume that  $\langle \tilde{M}_I^{\mathbf{q}} \Psi_{\mathbf{k}n} | \Psi_{\mathbf{q}+\mathbf{k}n'} \rangle$  only depends  $n$ ,  $n'$ ,  $\mathbf{k}$ , or  $\mathbf{k} + \mathbf{q}$  through the coefficients,  $(\alpha_{Ru}^{\mathbf{k}n})^* \alpha_{Ru}^{\mathbf{k}+\mathbf{q}n'}$ . Moreover, the core level energy is large and negative, and nearly independent of  $\mathbf{k}$  or  $n$ . Since the dominant contributions to  $\Pi$  will

come from coupling to low-lying states, we can approximate  $\varepsilon_{kn} - \varepsilon_{k'n'}$  by a constant, e.g.  $E_F - \varepsilon_{\text{core}}$ . These approximations are all modest but can vastly simplify the computation of  $\Pi^{\text{CORE}}$ .

The fact that the core spills out slightly from the augmentation region needs to be taken into account<sup>22</sup>. This can readily be accomplished by integrating the core and corresponding valence  $\varphi_l$  to a larger radius, and orthogonalizing  $\varphi_l$  to the core. Checks show that the adjustment to  $\phi_l$  is small unless the core is very shallow, in which case the core should be treated as a valence state.

### Comparison to PPGW

When the highest cores are put explicitly into the valence as Tiago et al. did, there is reasonable agreement between PPGW and our results for *sp* semiconductors. Comparison with the paper of Tiago et al. to Table II below shows that there is agreement at the  $\sim 0.1$  eV level in Si<sup>39</sup> and similar agreement is found for GaAs and Ge, with the PPGW results systematically higher than our results by  $\sim 0-0.1$  eV. Similarly, Fleszar and Hanke<sup>38</sup> calculated QPEs in the GWA for a variety of II-VI semiconductors, including the highest *s* and *p* cores in the valence. Their values are also in reasonable agreement with results presented in Table III (below), though the PPGW data are systematically higher by  $\sim 0.0-0.2$  eV. (Part of the discrepancy can be traced to contributions from high-lying *d* states, which are included in the present calculation using local orbitals.) Even when the high-lying *s* and *p* core states are included explicitly in the valence, it still seems to be the case that PPGW band gaps are systematically slightly larger (by  $\sim 0.1$  eV) in semiconductors than our *GW* predict.

Materials involving transition metals are rather more complicated. In a recent PPGW calculation, Marini, Onida and del Sole analyzed the QP valence bands of Cu<sup>40</sup>, comparing in some detail the occupied *d* bands to photoemission experiments. The LDA places the position of these levels approximately 0.5 eV closer to  $E_F$  than the experiments show. The authors find that the *d* bands narrow and shift downward by approximately 0.5 eV, bringing the PPGW *d* bands into excellent agreement with photoemission experiments. They report that the PPGW results depend rather dramatically on the treatment of the Cu core 3*s* and 3*p* levels: that it is necessary to include both states explicitly in the valence to obtain

reasonable results. They found that the correlation contribution  $\Sigma_c^{\text{core}}$  from these states shifts the  $d$  bands downward  $\sim 0.5$  eV.

We conducted a similar calculation using the present all-electron  $GW$ , and find a very different result. In our case, the  $GW$  correction to the LDA  $d$  bands is small—between 0 and 0.1 eV. Moreover, QPEs are essentially independent of how the Cu  $3p$  state is treated: the  $3d$  levels change by less than 0.05 eV when the Cu  $3p$  state is explicitly included in the valence (using a  $3p$  local orbital), as compared to being treated as core at the exchange-only level. The Cu  $3p$  state is rather deep, and the weak dependence on correlation contributions from it is consistent with the rule of thumb indicated above:  $Q_{\text{spill}} \approx 0.005$  electrons;  $\epsilon_{3p}^{\text{LDA}} \approx -70$  eV. In the Cu case, it appears likely that the main discrepancy between PPGW and our  $GW$  (whether  $d$  bands shift by 0.5 eV or not) originates in the discrepancies in  $\Sigma_c^{\text{core}}$ .

## VI. ADEQUACY OF GWA APPLIED TO A RANGE OF MATERIALS

In Ref. 10 Delaney et al. argued that GWA based on the LDA eigenfunctions and eigenvalues, is an adequate (or better) approximation than self-consistent  $GW$ . It is apparently the case that self-consistency worsens agreement with experiment for the Be atom. Moreover, Holm and von Barth<sup>41</sup> found that the valence bandwidth of the homogeneous electron gas is considerably worsened by self-consistency; similarly a self-consistent  $GW$  calculation Ku and Egiluz resulted in an overestimate of the valence bandwidth in Ge<sup>6</sup>. Thus, self-consistency of this type has shortcomings. On the other hand, even in simple materials such as  $sp$  semiconductors,  $GWA$  bandgaps based on LDA eigenvalues and eigenfunctions are *always* underestimated when properly calculated<sup>2,38</sup>. The  $GWA$  based on LDA is evaluated as a perturbation relative to LDA; thus the band gap can be poor if the LDA itself is poor. Thus, some kind of self-consistency is necessary to reduce the dependence on the starting point.

In this section, we consider three points about the  $GWA$  based on LDA, Eq. (6):

- (A) Use of the  $Z$  factor. We show that using  $Z = 1$  in Eq. (6) is a way to include partial self-consistency, and it should be a better approximation than including the  $Z$  factor.
- (B) Off-diagonal  $\Sigma$ . Eq. (6) is a perturbation treatment that involves only the diagonal matrix element of  $\Sigma$ . We consider the effect of the full  $\Sigma$  on the fundamental gap, and



also point to some consequences of the perturbation treatment.

(C) The adequacy of *GWA* is dependent on the adequacy of LDA. Even *GWA* with  $Z = 1$  fails for cases when the starting LDA is poor.

### A. $Z$ factor

Let us consider a partial kind self-consistency where only eigenvalues are updated: both eigenfunctions and  $W$  are unchanged from the LDA. This is a little different from the customary usual eigenvalue-only self-consistency, where eigenfunctions are frozen but  $W$  is updated. Updating eigenvalues widens semiconductor bandgaps. This reduces the screening, which causes  $W$  to increase, which in turn cause gaps to increase still more. Thus we expect that results from such the kind of partial self-consistency we are considering here should fall somewhere between the usual one-shot *GW* and the usual eigenvalue-only self-consistency. Partial self-consistency, while incomplete, should result in better QPEs than the standard 1-shot *GW*, since eigenvalues shift in the right direction. Appendix A evaluates how Eq. (6) gets modified for a model two-level system. The result is that this kind of self-consistency can be approximately realized by putting  $Z_{kn} = 1$  in Eq. (6). A different justification for omitting the  $Z$  factor emerged from a paper of Niquet and Gonze<sup>42</sup>, who calculated the interacting bandgap energy (within RPA) to obtain a correction to the Kohn-Sham bandgap energy. They found that the difference is essentially Eq. (6) with  $Z = 1$ .

The calculations in Table III support the argument that using  $Z=1$  is a better approximation than including  $Z$ : semiconductor bandgaps are in significantly better agreement with experiment. They continue to be smaller than experimental values, which can be qualitatively understood as follows. Using  $Z=1$  corresponds to updating  $G$ , but leaving  $W$  determined from the LDA eigenfunctions and eigenvalues. Because the gap is underestimated in the construction of  $\Pi$  and  $W$ ,  $\Pi$  is overestimated so that  $W$  is screened too strongly; thus  $\Sigma$  is too small. It is interesting, however, that QPEs evaluated with  $Z=1$  can be rather good at times because of a fortuitous cancellation of errors. We can refine self-consistency by updating  $W$  in a manner similar to the updating of  $G$ : that is using eigenvalues from Eq. (6) in the calculation of  $\Pi$ . However,  $\epsilon$  computed in the RPA omits excitonic effects. Inclusion of electron-hole correlations to  $\Pi$  (via e.g., ladder diagrams) increases  $\text{Im } \epsilon(\omega)$  for  $\omega$  in the vicinity of the gap for semiconductors. There is a concomitant increase in  $\text{Re } \epsilon(\omega)$

TABLE III: Fundamental gap, in eV. (For Gd, QPE correspond to the position of the majority and minority  $f$  levels relative to  $E_F$ ; for Cu QPE corresponds to the  $d$  level.) Low temperature experimental data were used when available. QPEs in the “ $GW$ ” column are calculated with usual  $GWA$  Eq. (6) and Eq. (7). In the “ $Z=1$ ” column the  $Z$  factor is taken to be unity. In the “ $\Sigma_{nn'}$ ” column the off-diagonal parts of  $\Sigma$  are included in addition to taking  $Z=1$ .  $k$ -meshes of  $8 \times 8 \times 8$   $k$  and  $6 \times 6 \times 6$  were used for cubic and hexagonal structures, respectively (symbol  $w$  indicates the wurtzite structure).  $GW$  calculations leave out spin-orbit coupling and zero-point motion effects. The former is determined from  $\Delta/3$ , where  $\Delta$  is the spin splitting of the  $\Gamma_{15v}$  level (in the zincblende structure); it is shown in the “ $\Delta/3$ ” column. Contributions to zero-point motion are estimated from Table 2 in Ref. 43 and are shown in the “ZP” column. The “adjusted” gap adds these columns to the true gap, and is the appropriate quantity to compare to  $GW$ .

	LDA	$GW$	$GW$	$GW$	Expt	$\Delta/3$	ZP	Adj
			$Z=1$	$\Sigma_{nn'}$				
C	4.09	5.48	5.74	5.77	5.49	0	0.34	5.83
Si	0.46	0.95 <sup>a</sup>	1.10	1.09	1.17	0.01	0.06	1.24
Ge	-0.13	0.66	0.83	0.83	0.78	0.10	0.05	0.93
GaAs	0.34	1.40	1.70	1.66	1.52	0.11	0.10	1.73
wAlN	4.20	5.83	6.24		6.28	0 <sup>b</sup>	0.20	6.48
wGaN	1.88	3.15	3.47	3.45	3.49	0 <sup>b</sup>	0.20	3.69
wInN	-0.24	0.20 <sup>a</sup>	0.33		0.69	0 <sup>b</sup>	0.16	0.85
wZnO	0.71	2.51	3.07	2.94	3.44	0 <sup>b</sup>	0.16	3.60
ZnS	1.86	3.21	3.57	3.51	3.78	0.03	0.10	3.91
ZnSe	1.05	2.25	2.53	2.55	2.82	0.13	0.09	3.04
ZnTe	1.03	2.23	2.55		2.39	0.30	0.08	2.77
CuBr	0.29	1.56	1.98	1.96	3.1	0.04	0.09 <sup>c</sup>	3.23
CdO	-0.56	0.10	0.22	0.15	0.84	0.01 <sup>b</sup>	0.05	0.90
CaO	3.49	6.02	6.62	6.50	$\sim 7$	0 <sup>b</sup>		
wCdS	0.93	1.98	2.24		2.50	0.03	0.07	2.60
SrTiO <sub>3</sub>	1.76	3.83	4.54	3.59	$\sim 3.3$			
ScN	-0.26	0.95	1.24	0.96	$\sim 0.9$	0.01 <sup>b</sup>		
NiO	0.45	1.1	1.6		4.3			
Cu <sup>d</sup>	-2.33	-2.35	-2.23	-2.18	-2.78			
Cu <sup>e</sup>	-2.33	-2.85	-2.73	-2.18	-2.78			
Gd <sup>↑</sup>	-4.6	-5.6	-6.2	-4.1	-7.9			
Gd <sup>↓</sup>	0.3	0.2	1.8	1.5	4.3			

<sup>a</sup>See Ref. 39

<sup>b</sup>LDA calculation

<sup>c</sup>Estimated from ZnSe

<sup>d</sup>Position of  $\Gamma_{15v}$   $d$  level, with  $E_F$  set to charge neutral point

for  $\omega \rightarrow 0$ , as is evident by the Kramers-Kronig relations; see e.g., Ref. 44. Errors resulting from the neglect of excitonic contributions to  $\epsilon$  partially cancel errors resulting from LDA eigenvalues, as shown by Arnaud and Alouani<sup>44</sup>. Thus,  $W$  calculated from LDA eigenvalues is not so bad in many cases because of this cancellation. Often  $\epsilon_\infty$  calculated from the LDA eigenvalues is better than  $\epsilon_\infty$  calculated from LDA eigenvalues shifted by a scissors operator to match the experimental band gap (See TABLE III in Ref. 44). This cancellation means that  $GW(Z=1)$  can be often be rather good, since  $W$  itself is also better than what would be obtained from (eigenvalue) self-consistency. Table III shows that the fundamental gap for  $GW(Z=1)$  is quite good for mostly-covalent semiconductors such as Si or GaAs, but that the agreement deteriorates as the ionicity increases.

### B. Off-diagonal contributions of $\Sigma$

The usual  $GWA$  in Eq. (6) does not include the off-diagonal contribution of  $\Sigma - V_{xc}^{LDA}$ . A simple way to take into account the contribution off-diagonal parts is to replace the energy-dependent matrix  $\Sigma$  with some static hermitian matrix  $V^{xc}$  as in the following, and to solve the eigenvalue problem, replacing  $V_{xc}^{LDA}$  in the LDA hamiltonian with this potential. We take

$$V^{xc} = \frac{1}{2} \sum_{ij} |\psi_i\rangle \{ \text{Re}[\Sigma(\epsilon_i)]_{ij} + \text{Re}[\Sigma(\epsilon_j)]_{ij} \} \langle \psi_j|, \quad (21)$$

for  $\Sigma$ . Here  $\text{Re}$  signifies the hermitian part, the eigenvalues  $\epsilon_i$  and the eigenfunctions  $\psi_i$  are in LDA. This  $V^{xc}$  is used in our QP self-consistent  $GW$  method<sup>11,12,13</sup>. This  $V^{xc}$  retains the diagonal part contribution as in Eq. (6) (we now consider  $Z=1$  case). From the perspective of the QP self-consistent  $GW$  method, including the off-diagonal  $\Sigma$  corresponds to the first iteration, and the LDA corresponds to the 0th iteration. Table III shows how the fundamental gap is affected by the off-diagonal parts of  $V^{xc}$  for selected semiconductors. Because the semiconductor eigenfunctions and density are already rather good, the off-diagonal contributions are small. Contributions from the off-diagonal part of  $V^{xc}$  significantly increase when eigenfunctions have significant  $d$  character (see SrTiO<sub>3</sub> and ScN in Table III). For correlated systems the effects can be rather dramatic; see Ref. 12 how the QPEs are affected by the off-diagonal parts of  $\Sigma$  in CeO<sub>2</sub>.

But even for the simple  $sp$  semiconductors, there can be a “band disentanglement prob-

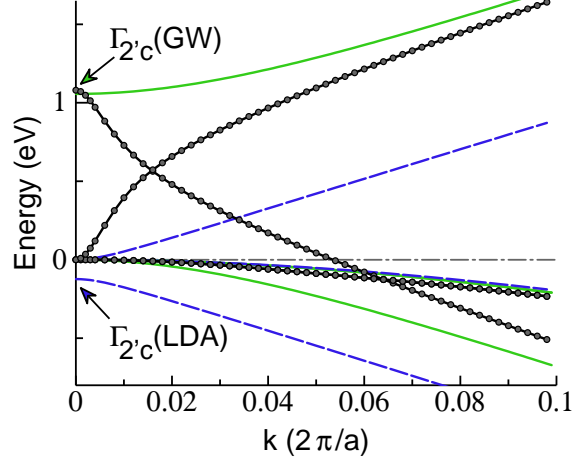


FIG. 6: Energy bands in Ge along [001] for small  $k$  within the *GWA*, using  $Z=1$ . Spin orbit coupling was omitted. Three approximations are compared: LDA (dashed blue line), *GW* in the diagonal- $\Sigma$  only approximation, Eq. (6) (black line with circles), and *GW* with  $\Sigma$  computed according to Eq. (21) (solid green line). In all three cases the three states of  $p$  character ( $\Gamma_{25'}$  symmetry) form the valence band maximum; this was taken to be the energy zero. The LDA predicts the conduction band, the  $\Gamma_{2'}$  state of  $s$  character, to be slightly negative, causing the energy bands to be wrongly ordered at  $\Gamma$ . For  $k > 0$ , the  $\Gamma_{25'}$  state of  $p_z$  symmetry couples to the  $\Gamma_{2'}$  state, and the two repel each other. Both kinds of *GW* put  $\Gamma_{2'c}$  at approximately the correct position, 1 eV. However, the diagonal-only *GW* must follow the topology of the LDA: the eigenvectors are unchanged from the LDA. Therefore the band starting out at  $\Gamma_{2'c}$  sweeps downward, while the  $p_z$  band starting out at  $\Gamma_{25'v}$  sweeps upward, and the two bands cross near  $k = 0.02$ . When the off-diagonal parts of  $\Sigma$  are included, these two bands repel each other as they should.

lem” as a consequence of the diagonal-only approximation. At times the LDA orders energy levels wrongly: in hcp Co, for example, it inverts the order of the minority  $\Gamma_5$  and  $\Gamma_3$  levels, which correspond to states of  $L_3$  and  $L_{2'}$  symmetry in the fcc structure. Wrong ordering of levels is a particularly serious difficulty for narrow-gap semiconductors such as Ge, InAs, InSb, and InN. Because the LDA underestimates bandgaps, the energy band structure around  $\Gamma$  has an inverted structure: the  $s$ -like conduction band of  $\Gamma_1$  symmetry (labeled as  $\Gamma_{2'}$  in the homopolar case) incorrectly falls below the  $p$ -like states of  $\Gamma_{25'}$  symmetry.

When the *GWA* is evaluated from Eq. (6), the energy bands retain the same connectivity as in the LDA, as Fig. 6 shows. Consequently the conduction band has a nonsensical negative

mass near  $\Gamma$ , and it crosses with one of the valence bands. The diagonal-only approximation cannot make Ge an insulator in principle, even though the levels are properly ordered at  $\Gamma$ . This problem is avoided if the off-diagonal parts of  $\Sigma$  are included, as Fig. 6 shows. The conduction-band effective mass in the latter case is computed to be  $m^* = 0.042m_0$ , in good agreement with a value of  $m^* = 0.038m_0$  estimated from magnetopiezoreflectance spectra<sup>45</sup>. This shows that the off-diagonal contributions of  $\Sigma$  are reasonably well described by Eq. (21).

### C. Dependence of *GWA* on the *LDA*

In general, *GWA* errors are rather closely tied to the quality of *LDA* starting point. In the covalent *sp* semiconductors C, Si and Ge, *GW* gaps are rather good for  $Z = 1$ . In the series Zn(Te,Se,S,O), the deviation between the *LDA* and experimental gap steadily worsens, and so does the *GW* gap. For ZnO, and even more so in CuBr, the *GW* gap falls far below experiment. For these simple *sp* materials, errors are related to their ionicity, which can be seen qualitatively as follows. As ionicity increases, the dielectric response becomes smaller; consequently the nonlocality missing from the *LDA* exchange-correlation potential<sup>46</sup> becomes progressively more important. Roughly speaking, a reasonable picture of electronic structure in *sp* systems resembles an interpolation between the *LDA*, which has no nonlocality in the exchange and underestimates gaps, and Hartree-Fock, which has nonlocality but wildly overestimates gaps because the nonlocal exchange is not screened. As ionicity increases the gap widens and the dielectric function decreases. As the screening is reduced the *LDA* becomes a progressively worse approximation. Thus, the *LDA* is not an adequate starting point for *GW* in such cases.

Discrepancies between *GW* and experiments become drastic when electronic correlations are strong. The *GWA* band gap for the antiferromagnetic-II NiO is far from experiment, and moreover the conduction band minimum falls at the wrong place (between  $\Gamma$  and  $X^{11}$ ). As Table III shows, the *LDA* puts *f* levels in Gd too close to  $E_F$ . *GWA* results are only moderately better: shifts in the Gd *f* level relative to the *LDA* are severely underestimated (see Table III).

The *LDA* fails even qualitatively in CoO: it predicts a metal with  $E_F$  passing through an itinerant band of *d* character. In this case, the *GWA* gives essentially meaningless results.

To get reasonable results it is essential to apply the *GWA* with a starting point that already has a gap. To get band gap for CoO in the single band picture, a non-local potential which breaks time-reversal symmetry is required, something which is not built into the local potential of the LDA. Similar problems occur with ErAs: the LDA predicts a very narrow minority  $f$  band straddling  $E_F$ , whereas in reality the minority  $f$  manifold is exchange-split into several distinct levels well removed from  $E_F$ <sup>47</sup>. *GWA* shifts the minority  $f$  levels only slightly relative to the LDA: the entire  $f$  manifold remains clustered in a narrow band at the Fermi level, appearing once again qualitatively similar to the LDA.

Generally speaking, the *GWA* (even *GWA*( $Z=1$ )) is reasonable only under limited circumstances—when the LDA itself is already reasonable.

## VII. CONCLUSIONS

To conclude, we have analyzed various possible sources of error in implementations of the *GWA*, using calculations based on an all-electron method with generalized Linear Muffin Tin Orbitals as a basis. We analyzed convergence in QPEs with the number unoccupied states  $N'$ : the rate of convergence for intermediate  $N'$  (where the LMTO energy bands were shown to precisely replicate APW bands), was qualitatively similar to, but roughly twice that of a PP analysis by Tiago, Ismail-Beigi, and Louie<sup>9</sup>. On the other hand, it closely tracked the convergence calculated by an LAPW+local orbitals method, which had a very similar LDA band structure. More generally, our *GWA* that properly subtracts  $V_{xc}^{LDA}$  calculated from the full density are in reasonable agreement with each other<sup>2,4,6,11,48</sup>; those that subtract valence density only<sup>5,7</sup> are also in reasonable agreement for cases such as Si and SiC where the cores are sufficiently deep. Our own experience suggests that the LDA treatment of core levels, where QPE are computed from Eq. (18), will be problematic for *GW*<sup>2</sup> unless the cores are very deep. Since a PP construction is an approximation whose justification is grounded in an all-electron theory, we should expect *GW* calculations based on an LDA PP should be similarly problematic. There is apparently a significant dependence on how cores are treated in PP implementations<sup>36,38,40,49</sup>, even in Si and Cu with their deep  $2p$  and  $3p$  cores.

We then presented a different analysis of convergence that is of particular importance for minimal-basis implementations, and argued that traditional measures (as given in Figs. 2 and

4) can be misleading. A finite size basis truncates the full Hilbert space of eigenfunctions in a different way than the truncation embodied in Figs. 2 and 4; and we showed that a suitably constructed minimal basis is sufficient to precisely describe the *GWA* QPE within 1 Ry or so of the Fermi level. We also showed that traditional linearization of basis functions, either explicit in an all-electron method or implicit through the construction of a pseudopotential, result in errors approximately independent of the size of basis. Addition of local orbitals to extend the linear approximation results in modest shifts in *sp* nitride and oxide compounds, and shifts of order 1-2 eV in transition-metal oxides.

We analyzed core contributions to the self-energy, and showed that an exchange-only treatment of the core is adequate in most cases. For all but the most shallow cores (such as Na *2p* and Ga *3d*), we showed that it is sufficient to include the core contribution to the polarization only; an approximate and rather painless implementation was suggested. These results can provide a framework for improved treatment of the core within a pseudopotential approximation.

Finally, we considered the adequacy of *GWA* based on the LDA, for different kinds of materials, and also Eq. (6) as an approximation to the *GWA*. We presented logical and numerical justifications that using  $Z=1$  generally gives better band gaps in insulators. In general inclusion of the off-diagonal part of  $\Sigma$  and some kind of self-consistency is essential to make the *GWA* a universally applicable and predictive tool. Taking into account both theoretical and practical aspects, the quasi-particle self-consistent *GW* scheme we have proposed<sup>11,12,13</sup> has the potential to be an excellent candidate for such a tool: it obviates some of the difficulties seen in the standard self-consistency, it no longer depends on the LDA, and it appears to predict QPEs in a consistently reliable way for broad classes of materials.

This work was supported by ONR contract N00014-02-1-1025. S. F. was supported by DOE, BES Contract No. DE-AC04-94AL85000. We thank the Ira A. Fulton High Performance Computing Initiative for use of their computer facilities.

## APPENDIX A: JUSTIFICATION FOR $Z = 1$ .

Let us consider a limited self-consistency within *GWA* as follows. We restrict self-consistency as follows:

1. We make only the QPE self-consistent. Eigenfunctions are constrained to be the LDA eigenfunctions.
2.  $W$  is assumed to be fixed. Thus only the eigenvalues entering into  $G$  are made self-consistent.

Under these assumptions, we can show that QPE are rather well approximated by Eq. (6) with  $Z = 1$ . To illustrate it, consider a two-states model whose LDA eigenvalues and eigenfunctions are given by  $\psi_1, \varepsilon_1$ , and  $\psi_2, \varepsilon_2$ , and the Fermi energy falls between these states:  $\varepsilon_2 > E_F > \varepsilon_1$ . Then the LDA Green's function is

$$G^{\text{LDA}}(\omega) = \frac{|\psi_1\rangle\langle\psi_1|}{\omega - \varepsilon_1 - i\delta} + \frac{|\psi_2\rangle\langle\psi_2|}{\omega - \varepsilon_2 + i\delta}. \quad (\text{A1})$$

After the limited self-consistency is attained, we will have eigenvalues:

$$G(\omega) = \frac{|\psi_1\rangle\langle\psi_1|}{\omega - E_1 - i\delta} + \frac{|\psi_2\rangle\langle\psi_2|}{\omega - E_2 + i\delta}, \quad (\text{A2})$$

where  $E_1$  is given by

$$E_1 = \varepsilon_1 + \text{Re}\langle\psi_1|\Sigma(E_1, [G]) - V_{\text{xc}}^{\text{LDA}}|\psi_1\rangle. \quad (\text{A3})$$

There is a similar equation for  $E_2$ . Note that  $\Sigma(E_1, [G])$  is calculated in GWA from  $G$  of Eq. (A2) at  $E_1$ .

As we can expect that  $W$  is dominated by diagonal terms  $W_1(\omega) = \langle\psi_1\psi_1|W(\omega)|\psi_1\psi_1\rangle$  and  $W_2(\omega) = \langle\psi_2\psi_2|W(\omega)|\psi_2\psi_2\rangle$ , we neglect other matrix elements of  $W(\omega)$ . Then  $\Sigma$  becomes

$$\begin{aligned} \text{Re}\langle\psi_1|(\Sigma(E_1, [G]))|\psi_1\rangle &= \text{Re} \int \langle\psi_1|iG(E_1 + \omega')W(\omega')|\psi_1\rangle d\omega' \\ &\approx \text{Re} \int \frac{iW_1(\omega') d\omega'}{E_1 + \omega' - E_1 - i\delta} \\ &= \text{Re} \int \frac{iW_1(\omega') d\omega'}{\varepsilon_1 + \omega' - \varepsilon_1 - i\delta} \\ &= \text{Re}\langle\psi_1|\Sigma(\varepsilon_1, [G^{\text{LDA}}])|\psi_1\rangle \end{aligned} \quad (\text{A4})$$

A similar equation applies for  $E_2$ . The energy shift  $E_1 \rightarrow \varepsilon_1$  entering into the evaluation  $\Sigma$  is exactly compensated by the energy shift in  $G \rightarrow G^{\text{LDA}}$ . Or equivalently using  $Z = 1$  is an approximate way to obtain self-consistency. Eq. (A4) corresponds Eq. (6) with  $Z = 1$ .

---

<sup>1</sup> L. Hedin, Phys. Rev. **139**, A796 (1965).



- <sup>2</sup> T. Kotani and M. van Schilfgaarde, Sol. State Commun. **121**, 461 (2002).
- <sup>3</sup> M. Usuda, N. Hamada, T. Kotani, and M. van Schilfgaarde, Phys. Rev. B **66**, 125101 (2002).
- <sup>4</sup> C. Friedrich, A. Schindlmayr, S. Blügel, and T. Kotani, in preparation.
- <sup>5</sup> N. Hamada, M. Hwang, and A. J. Freeman, Phys. Rev. B **41**, 3620 (1990), URL <http://link.aps.org/abstract/PRB/v41/p3620>.
- <sup>6</sup> W. Ku and A. G. Eguiluz, Phys. Rev. Lett. **89**, 126401 (2002).
- <sup>7</sup> S. Lebègue, B. Arnaud, M. Alouani, and P. E. Bloechl, Phys. Rev. B **67**, 155208 (2003).
- <sup>8</sup> Of the several all-electron implementations of the *GW* method that have been developed to date, some of them treat the core at the LDA level, and subtract the valence-only part of the LDA exchange correlation potential<sup>7</sup>. Thus, care must be taken when comparing different all-electron calculations. In the Si and SiC cases the cores are very deep, and it matters little whether only the valence electrons or all the electrons are included in the *GW* potential.
- <sup>9</sup> M. L. Tiago, S. Ismail-Beigi, and S. G. Louie, Phys. Rev. B **69**, 125212 (2004).
- <sup>10</sup> K. Delaney, P. García-González, A. Rubio, P. Rinke, and R. Godby, Phys. Rev. Lett. **93**, 249701 (2004).
- <sup>11</sup> S. V. Faleev, M. van Schilfgaarde, and T. Kotani, Phys. Rev. Lett. **93**, 126406 (2004).
- <sup>12</sup> M. van Schilfgaarde, T. Kotani, and S. Faleev (2006), to appear in Phys. Rev. Lett.. Preprint cond-mat/0510408 preprint.
- <sup>13</sup> A. N. Chantis, M. van Schilfgaarde, and T. Kotani, Physical Review Letters **96**, 086405 (pages 4) (2006), URL <http://link.aps.org/abstract/PRL/v96/e086405>.
- <sup>14</sup> The *GW* fundamental gap for Si was incorrectly quoted as 0.84 eV in Ref. 11. The correct value is 0.91 eV.
- <sup>15</sup> M. Methfessel, M. van Schilfgaarde, and R. A. Casali, in *Lecture Notes in Physics*, edited by H. Dreyse (Springer-Verlag, Berlin, 2000), vol. 535.
- <sup>16</sup> O. K. Andersen, Phys. Rev. B **12**, 3060 (1975).
- <sup>17</sup> E. Bott, M. Methfessel, W. Krabs, and P. C. Schmidt, J. Math. Phys. **39**, 3393 (1998).
- <sup>18</sup> P. E. Blochl, Phys. Rev. B **50**, 17953 (1994).
- <sup>19</sup> A recent LAPW-*GW* calculation by C.Friedrich, A.Schindlmayr, S.Blügel and T.Kotani (to appear in Phys. Rev. B), including eigenfunctions with about 300 valence bands, obtained a bandgap slightly larger (by  $\sim 0.04$  eV) than the results presented here, when similar input conditions for the *GW* calculation are used.

- <sup>20</sup> T. Kotani, M. van Schilfgaarde, and S. Faleev (2005), in preparation.
- <sup>21</sup> In the LDA a small amount of the envelope function remains inside the augmentation spheres, to handle incomplete  $l$  convergence of the augmentation functions. In the present *GW* implementation this feature is not retained, because of the nonlocal character of the potential. As a consequence wave function products must be augmented to higher  $l$  than in the LDA case.
- <sup>22</sup> In the *GW* scheme as we have currently implemented it, the LDA core states are approximated by truncating them outside the MT spheres, and scaling the part inside the MT sphere to conserve charge. An alternative would be to integrate the core wave function subject to the boundary condition that the value and slope vanish at the MT boundary. In either case, the core is not strictly orthogonal to the valence; this appears to be the primary source of error in the present treatment of the core. Experience with the more precise local orbitals treatment shows that this approximation is not serious at the “exchange-only” level. However their contribution to correlation is reliable only for relatively deep cores such as the Si  $2p$ .
- <sup>23</sup> F. Aryasetiawan and O. Gunnarsson, Phys. Rev. B **49**, 16214 (1994).
- <sup>24</sup> J. Rath and A. Freeman, Phys. Rev. B **11**, 2109 (1975).
- <sup>25</sup> Using the linear tetrahedron method, a mesh of  $6 \times 6 \times 6$  divisions (doubling the number of points in the energy denominator) resulted in an approximately rigid shift of +0.02 eV relative to a calculation with an  $8 \times 8 \times 8$  mesh, while a  $4 \times 4 \times 4$  mesh was found to overestimate the conduction bands by 0.10 eV. These shifts were approximately unchanged when varying, e.g., the basis set or the number of unoccupied states.
- <sup>26</sup> W. Ku and A. G. Eguiluz, Phys. Rev. Lett. **93**, 249702 (2004).
- <sup>27</sup> A. Yamasaki and T. Fujiwara, J. Phys. Soc. Japan **72**, 607 (2003).
- <sup>28</sup> We can treat the core state explicitly as valence states through the use of local orbitals, or solve for the core independently; see Sec. II. For a deep core such as the Si  $2p$  it matters little whether the core eigenfunctions are computed separately or generated through a local orbital, even with the approximate core treatment<sup>22</sup>. This is expected since the core level is very deep. Since the LDA eigenfunctions are represented completely differently in the two cases, the stability is a confirmation of the robustness of the method. For shallow cores with their larger radial extent, approximations in our present treatment of core states<sup>22</sup> do not enable us to distinguish true core contributions from artifacts of the implementation, so we use the local orbital approach here.

- <sup>29</sup> L. Steinbeck, A. Rubio, L. Reining, M. Torrent, I. White, and R. Godby, *Computer Physics Communications* **125**, 105 (2000).
- <sup>30</sup> We reiterate the present LMTO method has a key advantage in that it can be made small, and also highly precise when needed; see Fig. 1.
- <sup>31</sup> Comparing the two basis sets of Fig. 4, the LDA occupied eigenvalues  $\varepsilon_{\mathbf{k}n}$  and total energy differ by  $\sim 10^{-3}$  and  $\sim 10^{-2}$  eV respectively. Thus, even though the LDA eigenvalues used to generate  $\Sigma$  are nearly identical for small  $N'$ , the gap changes by  $\sim 0.01$  eV. In principle, both curves in Fig. 4 should converge to a common value as  $N'$  becomes small. That they deviate slightly is not a measure of convergence in the basis, but is connected with limitations to numerical precision in the method. It is apparently unavoidable because the eigenfunctions are represented in very different ways in the two basis sets: slight differences in them are responsible for the gap difference. Thus, the gap is  $\sim 0.01$  eV higher in the small basis case *both* for small  $N'$  and at their maximum  $N'$ : it is an indication that incompleteness of basis is not the dominant source of the discrepancy between the two basis sets. Apparently random changes in eigenvalues of order  $\pm 0.01$  eV are also seen in Fig. 5 (for a fixed choice of  $\{\varphi_{Ru}\}$ ) for a wide variety of basis sets. Similar discrepancies are also seen when comparing to the gap generated by an LAPW basis: with similar input conditions for the *GW* part—similar tolerances and approximately similar augmentation functions  $\{\varphi_{Ru}\}$ —the LAPW the gap falls  $\sim 0.04$  eV higher than those calculated by the present method<sup>19</sup>. Moreover, there is a slight dependence of the gap on augmentation radius: shrinking augmentation sphere volume by 30% has the effect of increasing the gap by  $\sim 0.01$  eV. Thus numerical accuracy is limited to order  $\sim 0.1$  eV or a little less for Si.
- <sup>32</sup> O. K. Andersen, T. Saha-Dasgupta, R. W. Tank, and G. K. C. A. O. Jepsen, in *Lecture Notes in Physics*, edited by H. Dreyse (Springer-Verlag, Berlin, 2000), vol. 535.
- <sup>33</sup> E. L. Shirley, L. Mitás, and R. M. Martin, *Phys. Rev. B* **44**, 3395 (1991).
- <sup>34</sup> E. L. Shirley and R. M. Martin, *Phys. Rev. B* **47**, 15 (1993).
- <sup>35</sup> E. L. Shirley, X. Zhu, and S. G. Louie, *Phys. Rev. Lett.* **69**, 2955 (1992).
- <sup>36</sup> E. L. Shirley, X. Zhu, and S. G. Louie, *Phys. Rev. B* **56**, 6648 (1997).
- <sup>37</sup> E. L. Shirley, R. M. Martin, G. B. Bachelet, and D. M. Ceperley, *Phys. Rev. B* **42**, 5057 (1990).
- <sup>38</sup> A. Fleszar and W. Hanke, *Phys. Rev. B* **71**, 045207 (2005).
- <sup>39</sup> QP levels calculated by ourselves in Ref. 2 did not have local orbitals included. Mostly for that reason, the QP levels are a little different from those cited here. Also, the gap in wurtzite

InN cited here is 0.17 eV larger than the 0.02 eV reported by Usuda<sup>48</sup>, who used LAPW eigenfunctions that did not have local orbitals. (Leaving out the N  $3p$  and In  $5d$  local orbitals, we obtained a gap of 0.01 eV with an LMTO basis in Ref. 2.) The basis sets used in the present calculations are substantially larger, and tolerances set tighter than in what Ref. 2 used. These changes make additional corrections of  $\sim 0.05$  eV. Finally the fundamental gap for Si was incorrectly tabulated as 0.84 eV in Ref. 11: the actual value for the basis used in that paper was 0.91 eV.

- <sup>40</sup> A. Marini, G. Onida, and R. D. Sole, Phys. Rev. Lett. **88**, 016403 (2002).
- <sup>41</sup> B. Holm and U. von Barth, Phys. Rev. B **57**, 2108 (1998).
- <sup>42</sup> Y. M. Niquet and X. Gonze, Phys. Rev. B **70**, 245115 (2004).
- <sup>43</sup> F. Manjón, M. Hernández-Fenollosa, B. Marí, S. Li, C. Poweleit, A. Bell, J. Menéndez, and M. Cardona, Eur. Phys. B **40**, 453 (2004).
- <sup>44</sup> B. Arnaud and M. Alouani, Phys. Rev. B **63**, 085208 (2001).
- <sup>45</sup> R. L. Aggarwal, Phys. Rev. B **2**, 446 (1970).
- <sup>46</sup> E. G. Maksimov, I. I. Mazin, S. Y. Savrasov, and Y. A. Uspenski, J. Phys. C **1**, 2493 (1989).
- <sup>47</sup> T. Komesu, H.-K. Jeong, J. Choi, C. N. Borca, P. A. Dowben, A. G. Petukhov, B. D. Schultz, and C. J. Palmstrom, Phys. Rev. B **67**, 035104 (2003).
- <sup>48</sup> M. Usuda, H. Hamada, K. Siraishi, and A. Oshiyama, Jpn. J. Appl. Phys. Lett. (part 2) **43**, L407 (2004).
- <sup>49</sup> M. Rohlfing, P. Kruger, and J. Pollmann, Phys. Rev. Lett. **75**, 3489 (1995).